Proportional Heading Control for Planar Navigation: The Chaplygin Beanie and Fishlike Robotic Swimming

Scott David Kelly Michael J. Fairchild Peter M. Hassing Phanindra Tallapragada

***Abstract*— We present a simple method for the coupled propulsion and steering of certain single-input planar vehicles. We demonstrate the applicability of this method to two distinct systems, one a hybridization of canonical systems from the mechanics literature and the other a fishlike robot. The first system is examined analytically, the second experimentally.**

I. INTRODUCTION

In a recent conference paper [1], the authors introduced an approach to coupled steering and propulsion for a class of single-input planar robotic vehicles exhibiting nonlinear dynamics. The class of vehicles in question encompasses both wheeled vehicles subject to noholonomic constraints and aquatic vehicles subject to forces associated with vortex shedding. The amenability of both to a single control method underscores a formal equivalence, previously explored by one of the authors in [2], between forces of constraint and lift-like hydrodynamic forces.

The vehicles considered in [1] and those considered in the present paper share a few key properties:

1) Each has a single internal degree of freedom, assumed to be under direct control;
2) The heading of each in the plane can be regulated, however indirectly, by manipulating this single degree of freedom;
3) Controlled variations in the heading of each additionally generate forward propulsion.

The fundamental control objective for each vehicle is to achieve — perhaps asymptotically — steady translation at a specified speed in a specified direction. The motion of the vehicle's internal degree of freedom need not cease as this objective is achieved, but must remain bounded in a physically appropriate sense. The solution of this control problem provides a basis for arbitrary planar navigation using a single input.

The control approach considered in [1] and in the present paper is simple and intuitive. A feedback loop is closed between the error in the vehicle's heading and the control input so that the behavior of the closed-loop system approximates that of a second-order linear system. The effective damping depends on a gain within the feedback loop. For a particular choice of gain, the heading of the vehicle will oscillate to a particular degree while stabilizing about the desired value. As a result of this oscillation, the vehicle will attain a particular forward speed in the desired direction.

For the systems considered in [1], the desired closed-loop behavior could be realized with nothing more than proportional feedback linking the heading to the control input. This was presented as a surprising result in [1], given the nonlinearity of the systems in question, but was substantiated only with simulations because of the unwieldy nature of the models presented.

In the present paper, we consider two additional systems for which proportional heading control is sufficient to achieve the desired closed-loop dynamics. These systems have been chosen to complement those discussed in [1]. Previously, we simulated the control of a rolling cart supporting a laterally translating mass; in Section II we explicitly analyze the control of a rolling cart supporting a spinning rotor. Previously, we simulated the control of a model for planar fishlike swimming; in Section III we test this controller with a real swimming robot.

II. THE CHAPLYGIN BEANIE

Research at the interface of analytical mechanics and nonlinear control theory has benefitted from the identification of certain canonical systems possessing just enough complexity to embody basic principles in their barest form. Two such systems are *Elroy's beanie* and the *Chaplygin sleigh*, both described below. Features of both systems combine in the dynamics of the *snakeboard* — itself an archetypical toy problem of persistent appeal [3], [4], [5], [6], [7] — but do so in the most elemental way in the single-input system we call the *Chaplygin beanie*.

A. Etymology

The problem of Elroy's beanie was invoked in [8], [9] to illustrate the concepts of *geometric phase* and *dynamic phase* in mechanics. Imagine a boy named Elroy to be floating in space, free from external forces.[1] Atop Elroy's head is a beanie to which a propeller is affixed in the manner popularized in caricatures of science-fiction fans.

If Elroy applies a torque to the propeller while holding his neck and body rigid, inducing the propeller to rotate relative to his head, then he himself will counter-rotate in accordance with the conservation of angular momentum about the propeller's axis. If the net angular momentum

Scott David Kelly, Peter M. Hassing, and Phanindra Tallapragada are with the Department of Mechanical Engineering and Engineering Science, University of North Carolina at Charlotte, Charlotte, NC 28223, USA.

Michael J. Fairchild is with the Department of Mathematics and Statistics, University of North Carolina at Charlotte, Charlotte, NC 28223, USA.

This material is based upon work supported by the National Science Foundation under grants CMMI-0822817, CMMI-1000652, and CMMI-1000656.

Correspondence should be directed to scott@kellyfish.net.

[1] But somehow able to survive in this state, at least for the duration of our *Gedankenexperiment*.

shared by Elroy and the propeller is zero, then Elroy's rotation is determined by the propeller's rotation in a manner independent of time-parametrization. Since the degree to which Elroy rotates when the propeller completes one full cycle depends only on the geometry of the path taken by the propeller through its configuration space, and not on the parametrization of this path, Elroy's rotation constitutes a geometric phase.

If the net angular momentum shared by Elroy and the propeller is nonzero, then the degree to which Elroy rotates as the propeller completes one full cycle will deviate from the geometric phase described above by an amount that depends in a simple way on the momentum in the system and on the period of rotation of the propeller. This discrepancy is the called the dynamic phase.[2]

The Chaplygin sleigh, comprising a rigid body moving in the plane subject to the requirement that a particular point on the body translate only along a single direction relative to a body-fixed frame, was studied a century ago by its namesake [11]. The system can be realized as a cart supported by two inertialess casters and a single inertialess wheel, with the assumption that the wheel can't slip laterally on the ground. In addition to appearing throughout standard modern treatments of nonholonomic mechanics [12], the Chaplygin sleigh is regularly revisited in the literature in modified form, whether on an inclined plane [13], submerged in an ideal fluid [14], or discretized [15].

The problem of steering the Chaplygin sleigh using external forces and torques has been considered recently [16], as has the problem of steering a modified sleigh fitted with a movable mass [17], [1]. In what follows, we consider the simultaneous steering and propulsion of a modified sleigh using an actuated rotor.

B. Modeling

Fig. 1 depicts the Chaplygin beanie. A cart is supported above a horizontal plane by two casters and a wheel. The plane of the wheel passes through the cart's center of mass, but the point at which the wheel makes contact with the ground is offset from the center of mass by a distance a. Mounted above the cart's center of mass is a balanced rotor. The rotational moment of inertia of the rotor relative to the center of mass is B (for "beanie"), the rotational moment of inertia of the cart relative to the center of mass is C, and the total mass in the system is m. The position of the center of mass relative to a stationary reference frame is specified by the pair (x, y) and the orientation of the system relative to this frame is specified by the angle θ. The rotation of the rotor relative to the cart is specified by the angle ϕ.

[2]The appeal of this example to the mechanician is increased by puppeteer Stan Freberg's claim that Albert Einstein was a fan of the televised puppet show *Time for Beany* in the early 1950s [10]. The title character conspicuously wore a propeller beanie like Elroy's. According to Freburg, who attributes this story to an unnamed Caltech physicist, Einstein once broke from a technical meeting with the explanation, "You will have to excuse me, gentlemen. It's *Time for Beany*." Disappointingly, the dynamics of Beany's Beanie-Cap Copter in the subsequent animated adaptation *Beany and Cecil* contradict the model from [8], [9].

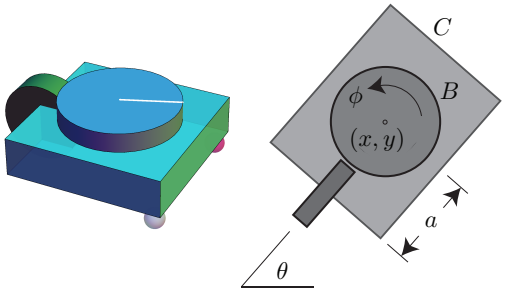

Fig. 1. The Chaplygin beanie.

We model the Chaplygin beanie as a constrained Lagrangian system, invoking the concept of nonholonomic reduction [18] to replace the trio of differential equations governing the evolution of $\dot{x}$, $\dot{y}$, and $\dot{\theta}$ with a pair of equations governing the evolution of the two-dimensional *nonholonomic momentum*. The stipulation that the wheel in Fig. 1 not slip laterally confines the evolution of the system's linear and angular momenta; the nonholonomic momentum is defined at each instant to comprise the components of linear and angular momentum that are allowed by the constraint.

The system's Lagrangian is given by the total kinetic energy

$$L = \frac{1}{2}m\left(\dot{x}^2 + \dot{y}^2\right) + \frac{1}{2}C\dot{\theta}^2 + \frac{1}{2}B\left(\dot{\theta} + \dot{\phi}\right)^2.$$

The no-slip constraint requires that

$$-\dot{x}\sin\theta + \dot{y}\cos\theta - a\dot{\theta} = 0; \tag{1}$$

this is equivalent to the requirement that the system's generalized velocity, understood as a vector tangent to the configuration manifold Q with coordinates (x, y, θ, ϕ), annihilate the constraint one form

$$\omega = -\sin\theta\, dx + \cos\theta\, dy - a d\theta$$

at every point $q \in Q$.

The manifold Q is given by the product $Q = SE(2) \times \mathbb{S}^1$, and the Lie group $SE(2)$ acts on Q by left translation in the first component of this product. It's straightforward to verify that L is invariant under the tangent lifted action and that ω is invariant under the cotangent lifted action, so that $SE(2)$ may be regarded as a symmetry group.

The nonholonomic momentum may be decomposed into scalar components in more than one way. Following [18], we fix a decomposition by choosing a pair of vector fields on Q to span the space

$$S_q = \mathcal{D}_q \cap T_q\,\mathrm{Orb}(q)$$

at each $q \in Q$, where $\mathcal{D}_q$ comprises all tangent vectors annihilated by ω and $T_q\,\mathrm{Orb}(q)$ denotes the space tangent to the orbit of the group action. We make the choice

$$S_q = \mathrm{span}\left\{-a\sin\theta\frac{\partial}{\partial x} + a\cos\theta\frac{\partial}{\partial y} + \frac{\partial}{\partial\theta}, \cos\theta\frac{\partial}{\partial x} + \sin\theta\frac{\partial}{\partial y}\right\}.$$

Flow along the first of these vector fields corresponds to rotation of the cart about the center of the wheel, below which the wheel makes its constrained contact with the ground. Flow along the second corresponds to longitudinal translation of the cart.

Each of the vector fields above constitutes the infinitesimal generator ξ_Q of the $SE(2)$ action corresponding to a particular (q-dependent) element ξ of the Lie algebra $\mathfrak{se}(2)$. The associated component J of the nonholonomic momentum is given by

$$J = \frac{\partial L}{\partial \dot{q}^i} \left(\xi_Q\right)^i, \tag{2}$$

where q^i is the ith coordinate on Q. Thus

$$\begin{aligned} J_{LT} &= m\dot{x}\cos\theta + m\dot{y}\sin\theta, \\ J_{RW} &= -m\dot{x}a\sin\theta + m\dot{y}a\cos\theta + (B+C)\dot{\theta} + B\dot{\phi} \end{aligned}$$

are the components of the nonholonomic momentum corresponding to longitudinal translation and rotation about the wheel, respectively. The latter expression can be simplified using (1) to obtain

$$J_{RW} = (ma^2 + B + C)\dot{\theta} + B\dot{\phi}.$$

The evolution of either component (2) of the nonholonomic momentum is governed by the differential equation

$$\dot{J} = \frac{\partial L}{\partial \dot{q}^i} \left[\frac{d\xi}{dt}\right]_Q^i.$$

Thus, after some algebra,

$$\begin{aligned} \dot{J}_{LT} &= \frac{ma\left(J_{RW} - B\dot{\phi}\right)^2}{\left(ma^2 + B + C\right)^2}, \\ \dot{J}_{RW} &= \frac{-a\left(J_{RW} - B\dot{\phi}\right)J_{LT}}{ma^2 + B + C}. \end{aligned} \tag{3}$$

C. Proportional Heading Control

In what follows, the rate of change of the angle ϕ will come into play but the angle itself will not. We denote the angular speed of the rotor by $\alpha = \dot{\phi}$. We analyze the behavior of the Chaplygin beanie when a torque is imparted to the rotor in proportion to the error in θ relative to some constant desired heading. Without loss of generality, we may assume the desired heading to correspond to $\theta = 0$.

The system of equations (3) was derived to involve only J_{LT}, J_{RW}, and $\dot{\phi}$, but our controller's explicit dependence on θ legitimizes our using the symbol $\dot{\theta}$ to simplify (3). The closed-loop system may therefore be written as

$$\begin{aligned} \dot{J}_{LT} &= ma\dot{\theta}^2 \\ \dot{J}_{RW} &= -a\dot{\theta}J_{LT} \\ \dot{\theta} &= \frac{J_{RW} - B\alpha}{ma^2 + B + C} \\ \dot{\alpha} &= k\theta. \end{aligned} \tag{4}$$

We observe immediately that $\dot{J}_{LT}$ cannot be negative. If the cart is initially at rest, then it can only roll forward thereafter, and must complete a turn in order to reverse direction.

We demonstrate that if J_{LT} is initially nonnegative, then the dynamics of (4) are such that

1) θ will tend to zero asymptotically over time;
2) J_{LT} will tend to a constant value determined (within some range) by the value of k.

We establish the first of these by constructing a Lyapunov function and the second by exploiting a conservation law. It's straightforward to extend our argument to the case in which J_{LT} is initially less than zero.

To streamline the discussion, we define the variables

$$\begin{aligned} r &= \frac{-aJ_{LT}}{ma^2 + B + C}, \\ w &= \frac{J_{RW}}{ma^2 + B + C}, \\ p &= \frac{J_{RW} - B\alpha}{ma^2 + B + C} \end{aligned}$$

and the constants

$$\begin{aligned} \gamma &= \frac{-ma^2}{ma^2 + B + C}, \\ \lambda &= \frac{kB}{ma^2 + B + C} \end{aligned}$$

so that (4) may be written in the form

$$\begin{aligned} \dot{r} &= \gamma p^2, \\ \dot{w} &= rp, \\ \dot{\theta} &= p, \\ \dot{p} &= rp - \lambda\theta. \end{aligned} \tag{5}$$

Note that γ is necessarily negative and that λ has the same sign as the feedback gain k. We choose k to be positive.

Consider the function

$$S = \frac{1}{2}\lambda\theta^2 + \frac{1}{2}p^2.$$

This function is positive definite and radially unbounded in the (θ, p) plane. As the system evolves according to (5),

$$\dot{S} = \lambda\theta\dot{\theta} + p\dot{p} = \lambda\theta p + p(rp - \lambda\theta) = rp^2.$$

Recall that J_{LT} must increase monotonically over time, so that r must decrease monotonically. If J_{LT} is initially zero but θ is nonzero, so that the rotor begins to spin, then J_{LT} will attain a positive value and r will attain a negative value. Whether J_{LT} is positive or zero initially, r will remain negative for all positive time, and $\dot{S}$ will remain negative as long as $p \neq 0$.

When a trajectory in the (θ, p) plane intersects the line $p = 0$, (5) indicates that $\dot{p}$ will be negative unless $\theta = 0$. Thus unless p and θ are simultaneously zero — indicating that the cart has attained the desired orientation and stopped rotating — p will attain a negative value and S will continue to decrease. It follows that the orientation $\theta = 0$ is globally asymptotically attractive.

It's straightforward to verify that the quantity

$$\Lambda = \frac{\left(J_{RW} - B\alpha\right)^2}{ma^2 + B + C} + kB\theta^2 + \frac{J_{LT}^2}{m}$$

is conserved by the flow of the closed-loop system (4), and that the sum of the first two terms to the right of the equality tends to zero over time. The asymptotic value of the cart's forward momentum can thus be determined by

$$\lim_{t\to\infty} J_{LT}^2 = m\Lambda(0) = D + kF,$$

where

$$D = m\frac{\left(J_{RW}(0) - B\alpha(0)\right)^2}{ma^2 + B + C} = m(ma^2 + B + C)\dot{\theta}(0)^2$$

and

$$F = mB(\theta(0))^2.$$

If $\theta \neq 0$ and $\dot{\theta} = 0$ initially, then k can be selected to achieve any positive value for $\lim_{t\to\infty} J_{LT}$. If $\theta \neq 0$ but $\dot{\theta} \neq 0$ initially, then k can be selected to achieve any positive value for $\lim_{t\to\infty} J_{LT}$ greater than a certain lower bound.

Fig. 2 depicts several snapshots from simulations of the system (4) with $\theta = 3\pi/2$ initially. In each case, the system is initially at rest. Within each panel, the position and orientation of the cart and rotor are shown at regular intervals in time. These intervals are the same for all three panels. For larger values of k, the system approaches its asymptotic state more rapidly, and α approaches a correspondingly larger constant value.

Although the cart appears to follow the same initial path in each of the three panels in Fig. 2, it doesn't follow the same path for all time, and both α and θ exhibit more pronounced reversals in sign as k is decreased. The trajectory of the cart is portrayed over a longer period of time for several values of k in Fig. 3.

III. FISHLIKE ROBOTIC SWIMMING

Fig. 4 depicts the self-propulsion of a single-degree-of-freedom planar hydrofoil under the influence of a proportional controller linking the foil's heading to the rate of change of its camber. The dynamics of the foil adhere to a model developed in [19] and summarized in [20]. The fluid is assumed to be inviscid; a Kutta condition [21] is applied periodically at the foil's trailing point to enable discrete vortex shedding. Shed vortices appear in Fig. 4 as colored dots in the foil's wake. The performance of this system under proportional heading control was examined previously in [22], [1].

At the start of the simulation depicted in Fig. 4, the foil was at rest, pointing directly to the right. At the instant shown, a step change in the desired heading has induced the orientation of the foil to oscillate about the new desired value, while corresponding oscillations in the foil's camber drive the foil forward. It was shown in [1] that the foil's asymptotic swimming speed can be dictated by the choice of feedback gain.[3] The closed-loop system in Fig. 4 is obviously less damped than the closed-loop system in Fig. 2, but oscillations in the foil's camber will diminish over time with the feedback gain set as it is in Fig. 4.

[3]An animation depicting the foil's response from rest to a sequence of two step changes in desired heading, the second involving a larger gain than the first, is visible online at `http://kellyfish.net/joukowski/p-control.mpg`.

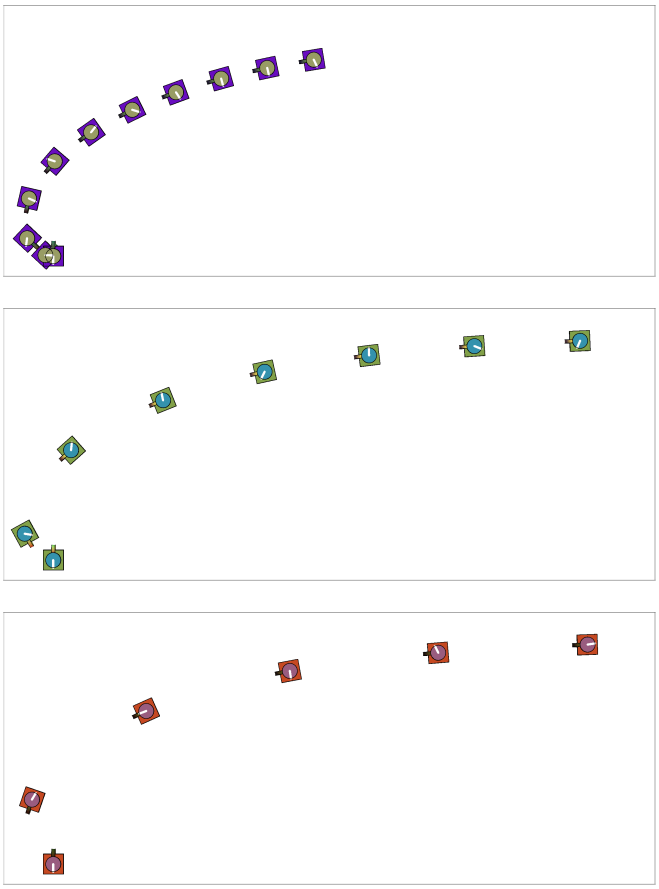

Fig. 2. Evenly timed snapshots of the Chaplygin beanie with $m = a = B = C = 1$ subject to the control law $\dot{\alpha} = k\theta$ for $k = 1$ (top), $k = 5$ (middle), and $k = 10$ (bottom).

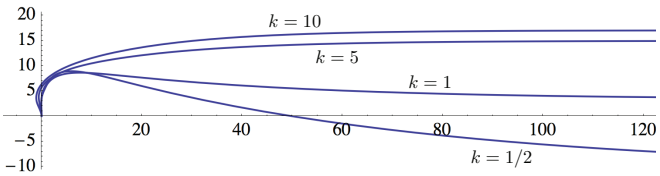

Fig. 3. Longer-time trajectories of the Chaplygin beanie from Fig. 2 corresponding to different values of k.

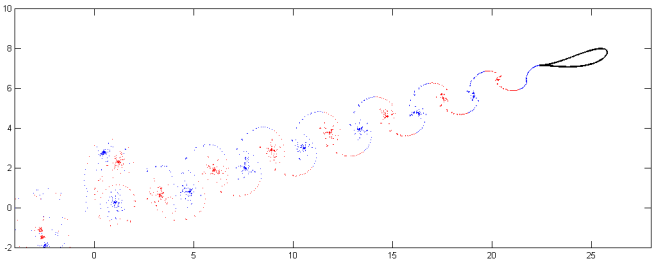

Fig. 4. Persistent propulsive oscillations in the camber of a free Joukowski foil under proportional heading control.

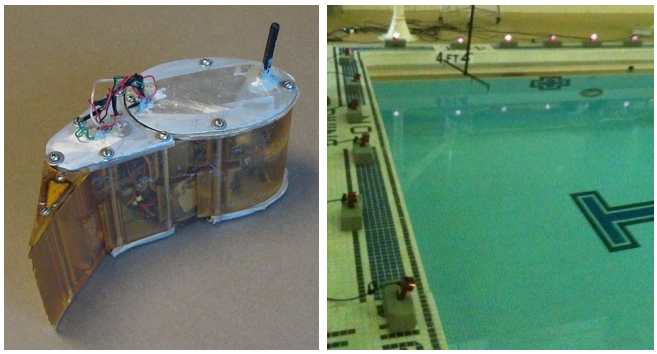

Fig. 5. Planar robotic hydrofoil and camera-based motion-tracking system.

A. Experimental Apparatus

The left-hand panel in Fig. 5 depicts a robotic version of the hydrofoil simulated in Fig. 4. The robot's outer shell comprises three rigid links; internal motors allow the two angles between these links to be varied independently. If the two angles are driven in phase, the camber of the robot may be considered a single shape parameter under control. The buoyancy and balance of the robot are tuned so that it floats upright in water with its upper face flush with the water's surface. The vertical antenna in the robot's bow remains above water to allows wireless communication with a stationary computer.

The right-hand panel in Fig. 5 depicts several cameras belonging to a Natural Point OptiTrack motion-capture system, aligned along the edges of a swimming pool in which the robot from the left-hand panel is free to swim. The motion-capture system informs the robot of its heading in real time; the robot's camber changes at a rate proportional to its deviation in heading from a piecewise-constant desired value.

B. Proportional Heading Control

A shortcoming of the model from Fig. 4 as a predictor of the dynamics of the robot from Fig. 5 is the model's omission of viscous forces other than those directly associated with localized vortex shedding. Applied to the robot, the proportional heading controller that allows the modeled hydrofoil to swim persistently allows the robot to swim only briefly. As oscillations in the hydrofoil's heading decay, the hydrofoil glides; as oscillations in the robot's heading decay, the robot comes to a halt.

As the feedback gain is increased in the case of the robot, a threshold is reached beyond which the closed-loop system isn't merely less damped, but is in fact unstable. Coupled with the fact that the robot's camber is limited mechanically, this instability is the key to inducing the robot to swim in a sustained way.

Fig. 6 depicts the heading of the robot subject to a controller that causes the oscillations in the robot's camber to be negatively damped. The heading initially deviates only a few degrees from the desired value of zero; the system responds with sustained oscillations of similar amplitude as the shape of the robot repeatedly reaches its opposite

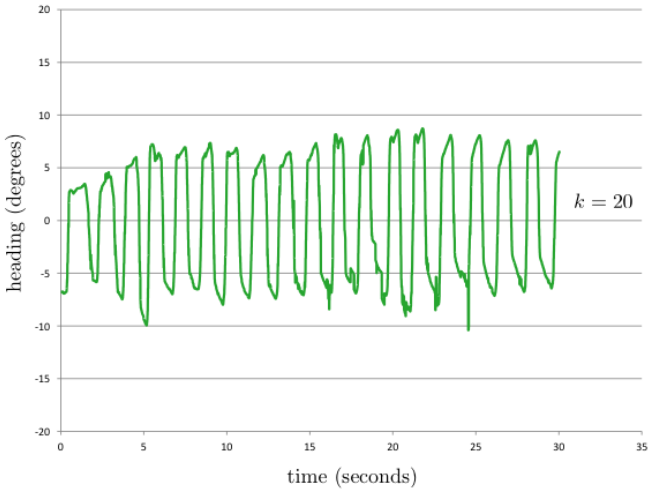

Fig. 6. Oscillations in the measured heading of the robot from Fig. 5, accelerating from rest, subject to a feedback controller inducing saturated unstable oscillations in the robot's camber.

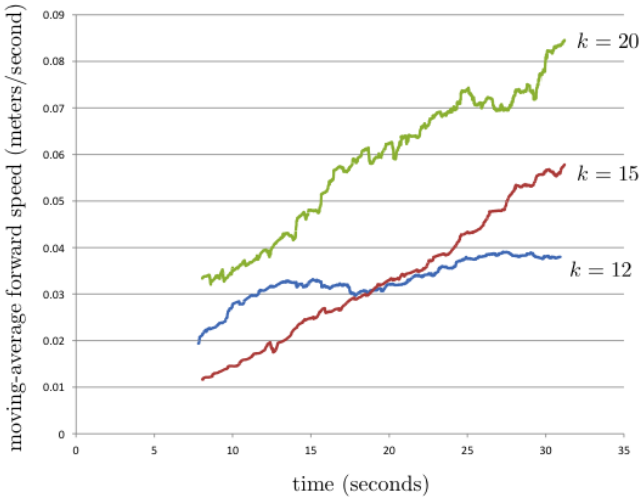

Fig. 7. Moving-average forward speed for the robot from Fig. 5, accelerating from rest, as a function of time for three different feedback gains. Data is depicted only after the accumulation of sufficiently many points for initial averaging.

extremes. The robot's forward speed increases toward a state in which thrust and drag are in balance.

Even when the feedback gain is such that oscillations in the robot's camber grow (modulo saturation) over time, the choice of gain determines the robot's forward speed. Fig. 7 depicts a moving average of the robot's forward speed as a function of time with the gain set at three different values. Each curve corresponds to an experiment in which the robot was initially at rest, rotated roughly five degrees from the heading specified when the controller was turned on at $t = 0$. In all three cases, the robot's camber is persistently saturated with each stroke. In no instance is the robot's acceleration smooth — nor was the surface of the pool along which the robot swam when data were collected — but it's clear that changes in the feedback gain affect the robot's average

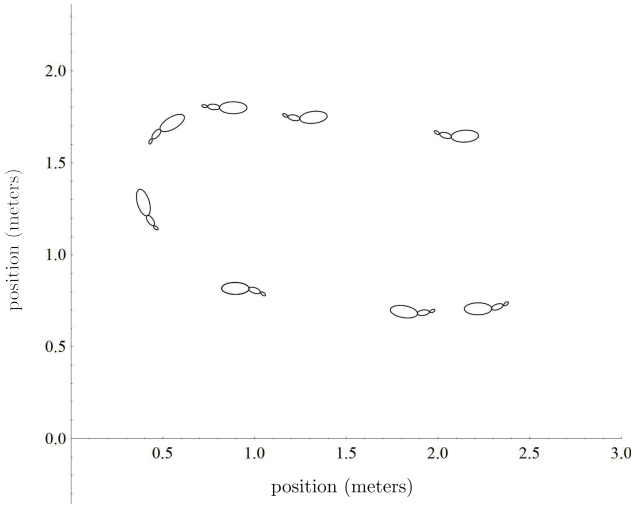

Fig. 8. Regularly timed snapshots of the robot from Fig. 5 maintaining one heading and then achieving and maintaining the opposite heading.

acceleration.[4]

Fig. 8 depicts a compound maneuver accomplished using unstable proportional heading control. The eight visible snapshots represent the configuration of the robot — portrayed to scale by a chain of ellipses — at equal intervals in time. At the beginning of the experiment, the robot was pointing to the left, aligned with the desired heading. Activating the controller caused the robot to respond to a small degree of drift by swimming to the left, maintaining its average heading. The desired heading was then changed by $180°$. The robot's camber remained saturated at one mechanical extreme as the robot coasted through the turn, then resumed oscillating as the robot resumed swimming with the new desired average heading.

IV. FUTURE WORK

The authors have presented analytical, computational, and experimental data recommending proportional heading control as a simple paradigm for nonlinear planar navigation, but the circumstances under which this approach is viable have yet to be characterized in a rigorous way. The idea of designing closed-loop systems to behave like damped oscillators is not new, and the authors look forward to linking the present work with topics like the formulation of PD control on Riemannian manifolds [23].

An open question concerning the Chaplygin beanie is whether or not the topology of the system's configuration manifold — whereby the headings $\theta = 2n\pi$ are equivalent for all integers n — can be exploited to achieve a measure of control over the final rotor speed at the conclusion of a maneuver like those depicted in Fig. 2. An algorithm to steer the system from rest to a state in which the asymptotic translational speed, heading, and rotor speed all matched prespecified values would convincingly illustrate the possibilities of single-input control.

[4]The initial superiority of the lowest gain to the intermediate gain underscores the fact that the optimal frequency for flapping-fin propulsion varies with translational speed.

REFERENCES

[1] M. J. Fairchild, P. M. Hassing, S. D. Kelly, P. Pujari, and P. Tallapragada, "Single-Input Planar Navigation via Proportional Heading Control Exploiting Nonholonomic Mechanics or Vortex Shedding," in *Proceedings of the ASME Dynamic Systems and Control Conference*, 2011.

[2] S. D. Kelly and R. B. Hukkeri, "Mechanics, Dynamics, and Control of a Single-Input Aquatic Vehicle With Variable Coefficient of Lift," *IEEE Transactions on Robotics*, vol. 22, no. 6, pp. 1254–1264, 2006.

[3] F. Bullo and A. D. Lewis, "Kinematic Controllability and Motion Planning for the Snakeboard," *IEEE Transactions on Robotics and Automation*, vol. 19, no. 3, pp. 494–498, 2003.

[4] V. Duindam, G. Blankenstein, and S. Stramigioli, "Port-Based Modeling and Analysis of Snakeboard Locomotion," in *Proceedings of the 16th International Symposium on Mathematical Theory of Networks and Systems*, 2004.

[5] A. S. Kuleshov, "Further Development of the Mathematical Model of a Snakeboard," *Regular and Chaotic Dynamics*, vol. 12, no. 3, pp. 321–334, 2007.

[6] A. R. Asnafi and M. Mahzoon, "Some Flower-like Gaits in the Snakeboard's Locomotion," *Nonlinear Dynamics*, vol. 48, no. 1–2, pp. 77–89, 2007.

[7] E. Shammas and M. de Oliveira, "An Analytic Motion Planning Solution for the Snakeboard," in *Proceedings of Robotics: Science and Systems*, 2011.

[8] J. E. Marsden, R. Montgomery, and T. S. Ratiu, "Reduction, Symmetry, and Phases in Mechanics," *Memoirs of the American Mathematical Society*, vol. 436, 1990.

[9] J. E. Marsden, *Lectures on Mechanics*. Cambridge University Press, 1992.

[10] S. Freburg, *It Only Hurts When I Laugh*. Crown, 1988.

[11] S. A. Chaplygin, "On the Theory of Motion of Nonholonomic Systems. The Theorem on the Reducing Multiplier," *Matematicheskii Sbornik*, vol. 28, no. 1, 1911.

[12] A. M. Bloch, *Nonholonomic Mechanics and Control*. Springer Verlag, 2003.

[13] A. V. Borisov and I. S. Mamaev, "The Dynamics of a Chaplygin Sleigh," *Journal of Applied Mathematics and Mechanics*, vol. 73, no. 2, pp. 156–161, 2009.

[14] Y. N. Fedorov and L. C. García-Naranjo, "The Hydrodynamic Chaplygin Sleigh," *Journal of Physics A: Mathematical and Theoretical*, vol. 43, no. 434013, 2010.

[15] M. J. Coleman and P. Holmes, "Motions and Stability of a Piecewise Holonomic System: The Discrete Chaplygin Sleigh," *Regular and Chaotic Dynamics*, vol. 4, no. 2, pp. 55–77, 1999.

[16] A. C. B. Antunes, C. Sigaud, and P. C. G. de Moraes, "Controlling Nonholonomic Chaplygin Systems," *Brazilian Journal of Physics*, vol. 40, no. 2, 2010.

[17] J. Osborne and D. V. Zenkov, "Steering the Chaplygin Sleigh by a Moving Mass," in *Proceedings of the 44th IEEE Conference on Decision and Control and European Control Conference*, 2005, pp. 1114–1118.

[18] A. M. Bloch, P. S. Krishnaprasad, J. E. Marsden, and R. M. Murray, "Nonholonomic Mechanical Systems with Symmetry," *Archive for Rational Mechanics and Analysis*, vol. 136, pp. 21–99, 1996.

[19] H. Xiong, "Geometric Mechanics, Ideal Hydrodynamics, and the Locomotion of Planar Shape-Changing Aquatic Vehicles," Ph.D. dissertation, University of Illinois at Urbana-Champaign, 2007.

[20] S. D. Kelly and H. Xiong, "Self-Propulsion of a Free Hydrofoil with Localized Discrete Vortex Shedding: Analytical Modeling and Simulation," *Theoretical and Computational Fluid Dynamics*, vol. 24, no. 1, pp. 45–50, 2010.

[21] S. Childress, *Mechanics of Swimming and Flying*. Cambridge University Press, 1981.

[22] S. D. Kelly and P. Pujari, "Propulsive Energy Harvesting by a Fishlike Vehicle in a Vortex Flow: Computational Modeling and Control," in *Proceedings of the 49th IEEE Conference on Decision and Control*, 2010.

[23] F. Bullo and R. M. Murray, "Tracking for Fully Actuated Mechanical Systems: A Geometric Framework," *Automatica*, vol. 35, no. 1, pp. 17–34, 1999.